



Global Biogeochemical Cycles

RESEARCH ARTICLE

10.1002/2016GB005541

Key Points:

- Surface ocean partial pressure of carbon dioxide ($p\text{CO}_{2\text{sw}}$) is calculated from pH on biogeochemical profiling floats
- The relative standard uncertainty in float $p\text{CO}_{2\text{sw}}$ estimates is 2.7% (or 11 μatm at $p\text{CO}_{2\text{sw}}$ of 400 μatm)
- For the first time extensive wintertime $p\text{CO}_{2\text{sw}}$ values are obtained in the Southern Ocean showing higher values than previous estimates

Supporting Information:

- Supporting Information S1

Correspondence to:

N. L. Williams,
nancy.williams@oregonstate.edu

Citation:

Williams, N. L., et al. (2017), Calculating surface ocean $p\text{CO}_2$ from biogeochemical Argo floats equipped with pH: An uncertainty analysis, *Global Biogeochem. Cycles*, 31, doi:10.1002/2016GB005541.

Received 3 OCT 2016

Accepted 1 MAR 2017

Accepted article online 3 MAR 2017

Calculating surface ocean $p\text{CO}_2$ from biogeochemical Argo floats equipped with pH: An uncertainty analysis

N. L. Williams¹ , L. W. Juranek¹, R. A. Feely², K. S. Johnson³ , J. L. Sarmiento⁴ , L. D. Talley⁵ , A. G. Dickson⁵ , A. R. Gray⁴ , R. Wanninkhof⁶ , J. L. Russell⁷ , S. C. Riser⁸, and Y. Takeshita³

¹College of Earth, Ocean, and Atmospheric Sciences, Oregon State University, Corvallis, Oregon, USA, ²Pacific Marine Environmental Laboratory, National Oceanic and Atmospheric Administration, Seattle, Washington, USA, ³Monterey Bay Aquarium Research Institute, Moss Landing, California, USA, ⁴Program in Atmospheric and Oceanic Sciences, Princeton University, Princeton, New Jersey, USA, ⁵Scripps Institution of Oceanography, University of California, San Diego, La Jolla, California, USA, ⁶Atlantic Oceanographic and Meteorological Laboratory, National Oceanic and Atmospheric Administration, Miami, Florida, USA, ⁷Department of Geosciences, University of Arizona, Tucson, Arizona, USA, ⁸School of Oceanography, University of Washington, Seattle, Washington, USA

Abstract More than 74 biogeochemical profiling floats that measure water column pH, oxygen, nitrate, fluorescence, and backscattering at 10 day intervals have been deployed throughout the Southern Ocean. Calculating the surface ocean partial pressure of carbon dioxide ($p\text{CO}_{2\text{sw}}$) from float pH has uncertainty contributions from the pH sensor, the alkalinity estimate, and carbonate system equilibrium constants, resulting in a relative standard uncertainty in $p\text{CO}_{2\text{sw}}$ of 2.7% (or 11 μatm at $p\text{CO}_{2\text{sw}}$ of 400 μatm). The calculated $p\text{CO}_{2\text{sw}}$ from several floats spanning a range of oceanographic regimes are compared to existing climatologies. In some locations, such as the subantarctic zone, the float data closely match the climatologies, but in the polar Antarctic zone significantly higher $p\text{CO}_{2\text{sw}}$ are calculated in the wintertime implying a greater air-sea CO_2 efflux estimate. Our results based on four representative floats suggest that despite their uncertainty relative to direct measurements, the float data can be used to improve estimates for air-sea carbon flux, as well as to increase knowledge of spatial, seasonal, and interannual variability in this flux.

Plain Language Summary The Southern Ocean is a key player in the global flow of carbon, yet it is hard to reach, and there are relatively few measurements there, especially in winter. Measuring the amount of carbon dioxide gas in seawater is key to advancing our understanding of the Southern Ocean. More than 74 robotic floats that use sensors to measure seawater properties have been deployed throughout the Southern Ocean, and each has a lifetime of around 5 years. It is currently not possible to directly measure carbon dioxide gas from these floats; however, it is possible to estimate carbon dioxide from things that the float can measure, like pH, a measure of ocean acidity. Here surface ocean carbon dioxide is estimated from several floats and compared to two ship-based estimates. In some locations, the floats closely match the existing estimates, but in other locations the floats see significantly higher surface ocean carbon dioxide in the wintertime, reinforcing the idea that the Southern Ocean's role in the global carbon cycle needs a closer look. Our results show that despite not measuring carbon dioxide directly, these floats will help scientists learn a lot about the Southern Ocean's part in the global flow of carbon.

1. Background

As anthropogenic carbon dioxide (CO_2) from fossil fuel burning and land use changes continues to build up in our atmosphere, the ocean has mediated the atmospheric increase by absorbing about 26% of emissions over the timeframe 2006–2015 [Le Quéré et al., 2016]. This oceanic sink for anthropogenic CO_2 is not equally distributed throughout the world oceans but is strongest in areas of deep and intermediate water formation such as the North Atlantic and the Southern Ocean, with the Southern Ocean accounting for around half of the total oceanic uptake [Frölicher et al., 2015]. Understanding how this anthropogenic CO_2 uptake occurs against the background of natural carbon fluxes is critical for understanding modern ocean changes as well as for improving climate modeling and projection.

The ocean takes up or releases CO_2 when there is a difference between the surface ocean partial pressure of CO_2 ($p\text{CO}_{2\text{sw}}$) and the atmospheric partial pressure of CO_2 ($p\text{CO}_{2\text{a}}$). The flux (F_{CO_2}) of carbon between the atmosphere and the ocean can be estimated using the following bulk formula:

$$C_{\text{CO}_2} = kK_0(p\text{CO}_{2\text{sw}} - p\text{CO}_{2\text{a}}) \quad (1)$$

where k is the gas transfer velocity (typically expressed as a function of wind speed) and K_0 is the solubility of CO_2 in seawater as a function of seawater temperature (T) and salinity (S). Because the atmosphere is zonally well mixed, the $p\text{CO}_{2\text{a}}$ at any point over the Southern Ocean is nearly equal to the atmospheric CO_2 measured at a land-based observatory such as the Cape Grim Station (available from <http://www.csiro.au/greenhouse-gases>) for the Southern Hemisphere, corrected for local sea level pressure and the vapor pressure of water as a function of surface ocean T and S . Historically, for purposes of determining air-sea CO_2 fluxes the $p\text{CO}_{2\text{sw}}$ is measured directly along with T and S using shipboard underway systems or moored systems. These underway and moored $p\text{CO}_{2\text{sw}}$ measurements have been favored, as no other truly autonomous systems exist. Moreover, direct $p\text{CO}_{2\text{sw}}$ measurements at in situ T have been deemed more accurate for assessment of air-sea flux than either the discrete bottle $p\text{CO}_{2\text{sw}}$ sampling method, in which samples are warmed to laboratory temperature before processing, or calculating $p\text{CO}_{2\text{sw}}$ with a carbonate system calculator such as CO2SYS [Lewis and Wallace, 1998; van Heuven *et al.*, 2011] using discrete measurements of any two of the other carbonate system parameters (total alkalinity (TA), pH, or dissolved inorganic carbon (DIC)).

The seasonality and interannual variability in F_{CO_2} is not well understood in the Southern Ocean owing to sparse observations, particularly in the austral winter. This lack of observations limits efforts to quantify annual fluxes, as well as estimates of how F_{CO_2} might change in the future. There have been several community efforts to compile high-quality measurements of $p\text{CO}_{2\text{sw}}$, and to date these compilations have been limited to direct measurements from drifter, shipboard, or moored systems. The most recent effort, the Surface Ocean CO_2 Atlas, version 4 (SOCATv4) [Bakker *et al.*, 2016], includes 18.5 million $f\text{CO}_{2\text{sw}}$ ($p\text{CO}_{2\text{sw}}$ corrected for the nonideal behavior of CO_2) values globally covering the years 1957–2015. Despite the large number of observations, the data set is spatially, temporally, and seasonally biased, especially in the Southern Ocean. Spatial biases arise because most Southern Ocean voyages are reoccupations of supply routes to Antarctic bases or of repeat hydrographic lines leaving large swaths of the Southern Ocean completely unsampled (Figure 1a). Seasonal biases occur because the Southern Ocean is difficult to access especially during austral winter when dangerous weather systems are frequent and when sea ice and icebergs may extend as far north as 50°S latitude. When comparing the distribution of SOCATv4 data from only austral winter (July–September; Figure 1b) with all Southern Ocean observations (Figure 1a), this seasonal bias becomes apparent.

From such data compilations researchers have developed data products for surface ocean $p\text{CO}_{2\text{sw}}$ and for F_{CO_2} such as the global monthly climatologies presented by Takahashi *et al.* [2009, 2014] and the global monthly gridded data product presented by Landschützer *et al.* [2014, 2015]. Takahashi *et al.* [2014] used this $p\text{CO}_{2\text{sw}}$ climatology combined with estimates of alkalinity to develop global monthly surface climatologies for pH, DIC, and the saturation states of aragonite and calcite. Efforts are taken to minimize the effects that spatial and temporal biases in the data have on these climatologies, but in much of the Southern Ocean the variability is large, the data are sparse, and such biases are unavoidable.

The Southern Ocean Carbon and Climate Observations and Modeling (SOCCOM) project (<http://soccom.princeton.edu>) aims to fill these observational gaps by deploying approximately 200 biogeochemical profiling floats over 5 years. Now in year three, the project has deployed more than 74 floats (Figure 1c). These floats are different from traditional Argo floats in that many include ice avoidance software and all carry some combination of additional biogeochemical sensors (pH, nitrate, oxygen, fluorescence, and backscattering). The measurement of pH is of special significance; when well calibrated, this can allow the calculation of $p\text{CO}_{2\text{sw}}$ to high precision using existing algorithms for TA that are based on other float-measured parameters (T , S , pressure (P), and O_2) [e.g., Carter *et al.*, 2016]. With current measurement accuracies the uncertainty of calculating $p\text{CO}_{2\text{sw}}$ from TA and pH is significantly smaller than calculating it from TA and DIC [Dickson and Riley, 1978]. The focus of this manuscript is to assess the uncertainties that result when these profiling float data are used to calculate $p\text{CO}_{2\text{sw}}$.

2. Methods

To calculate $p\text{CO}_{2\text{sw}}$ from SOCCOM biogeochemical floats, the in situ pH measured using a Deep-sea DuraFET pH sensor [Johnson *et al.*, 2016] is combined with an algorithm-based estimate for TA. The CO2SYS MATLAB program [van Heuven *et al.*, 2011; available from <http://cdiac.ornl.gov/ftp/co2sys>], the equilibrium constants

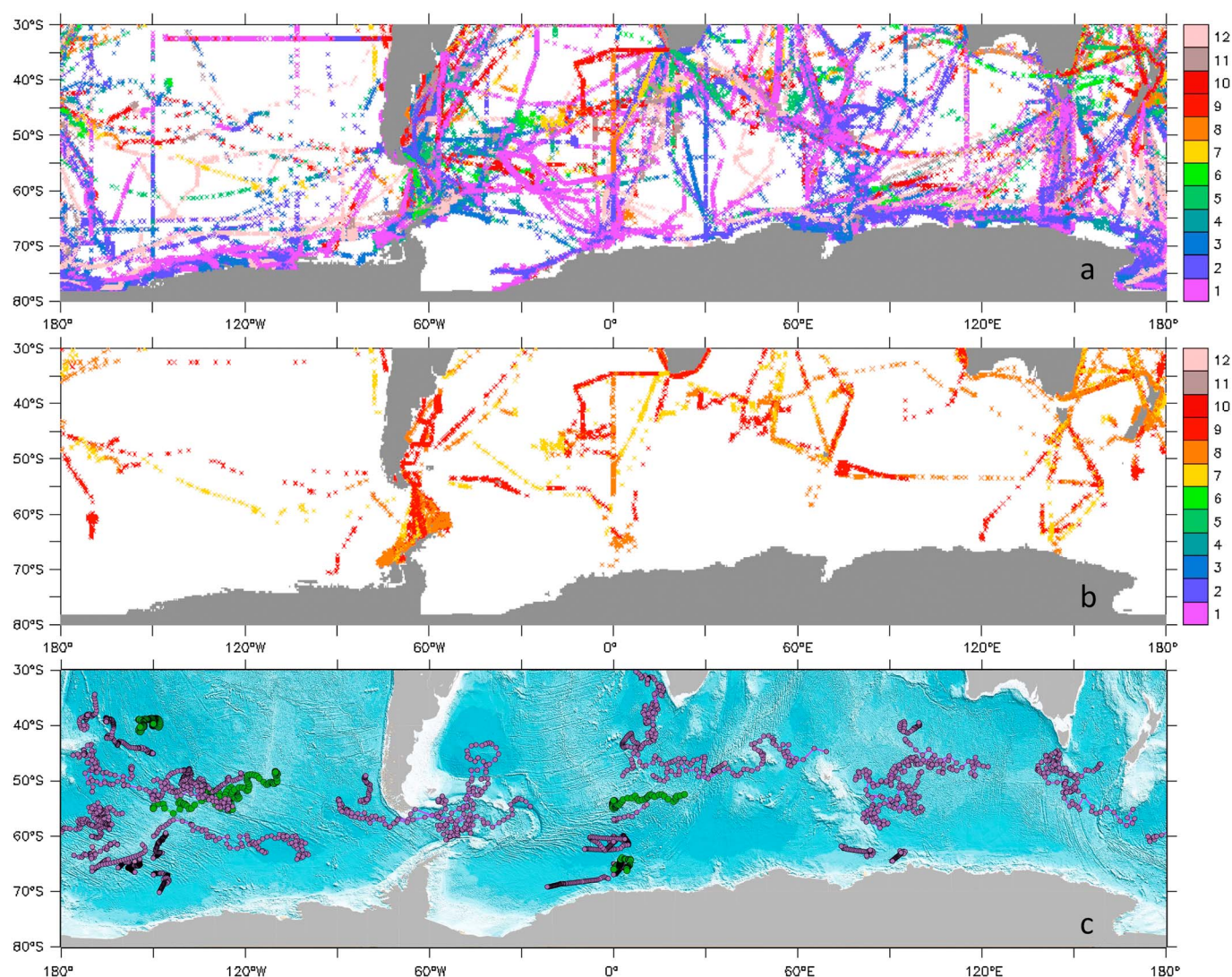


Figure 1. SOCATv4 $p\text{CO}_{2\text{sw}}$ data [Bakker *et al.*, 2016] south of 30°S colored by month for years 1957–2015 (a) for all months and (b) for only austral winter months (July–September). (c) A map of trajectories of all SOCCOM floats from 26 March 2014 to 4 January 2017 with the floats used in this study colored in green.

of Lueker *et al.* [2000], Dickson [1990], and Perez and Fraga [1987], and the boron to salinity ratio of Lee *et al.* [2010] as recommended by A. Dickson [Wanninkhof *et al.*, 2016a] were used for this analysis, and pH is in situ on the total hydrogen ion concentration scale. For the remainder of this manuscript the notation $X(Y, Z)$ is used to indicate that carbonate system parameter X was calculated using CO2SYS with inputs of Y and Z .

The SOCCOM float pH sensor data are adjusted in near-real time using an empirical algorithm for in situ pH based on T , S , P , and O_2 [Williams *et al.*, 2016]. The following steps describe the pH sensor calibration adjustment process: (1) convert shipboard bottle pH ($T = 25^\circ\text{C}$ and $P = 0$ dbar) to in situ pH (at conductivity-temperature-depth (CTD) T and P), (2) determine multiple linear regression (MLR) algorithm [Williams *et al.*, 2016] to estimate in situ pH as a function of T , S , P , and O_2 using in situ pH from depths between 1000 and 2000 m determined from recent shipboard bottle measurements (2011 to present) from Southern Ocean and SOCCOM deployment cruises, (3) apply MLR algorithm to float-measured T , S , P , and O_2 to obtain MLR in situ pH estimate, (4) adjust Deep-sea DuraFET pH sensor reference potential [Johnson *et al.*, 2016] to match 1500 m sensor in situ pH to MLR in situ pH estimate using either a one-time offset correction or a time-dependent drift correction (units of year^{-1}), (5) apply new calibration to entire float profile.

A minimum number of adjustments are made to keep the float pH within 0.005 of the MLR algorithm estimate; the method is described in more detail by Johnson *et al.* [2016], Wanninkhof *et al.* [2016a], and

Table 1. Float pH Sensor Quality Control Adjustment Record

SOCCOM Float ID	Deployment Calibration CTD Station	Approximate Days Since Deployment	Adjustment for Offset ^a	Adjustment for Drift ^b (year ⁻¹)	Cumulative Adjustment ^a
9254	station 53 of P16S 2014 GO-SHIP cruise; 20 April 2014	0	−0.0217	0	−0.0217
		6	0.029	0.125	0.0073
		43	0.002	−0.028	0.0220
		291	0	0	0.0030
9031	station 27 of P16S 2014 GO-SHIP cruise; 11 April 2014	0	−0.0237	0	−0.0237
		5	−0.033	0	−0.0567
		11	0.013	−0.135	−0.0437
		187	0	−0.036	−0.1088
		339	−0.004	−0.005	−0.1277
		582	0	0	−0.1311
9096	station 12 of A12/PS89; 10 Dec 2014	0	−0.2770	0	−0.2770
		10	0.0500	0	−0.2270
		70	−0.0130	−0.059	−0.2400
		190	−0.002	−0.078	−0.2614
		390	0.002	−0.036	−0.3021
		670	0	0	−0.3297
9099 ^c	station 78 of A12/PS89; 19 Jan 2015	0	−0.0097	0	−0.0097
		170	0.0000	0	−0.0097
		240	−0.0130	0.017	−0.0227
		350	−0.002	−0.005	−0.0196
		500	0.003	0	−0.0186
		640	−0.0090	0	−0.0276

^aOffset is negative when sensor pH is low compared to MLR pH estimate.^bDrift rate is negative when sensor pH is drifting lower.^cFloat 9099 was conditioned in flowing seawater before deployment.

Williams *et al.* [2016]. When appropriate, time-dependent drift corrections are applied to decrease bias in the pH measurements as the sensor drifts over time. Table 1 outlines the adjustments that have been made to the four SOCCOM float pH sensors utilized in the discussion. Offset adjustments are additive and cumulative, whereas drift adjustments only apply until they are overridden by a subsequent drift adjustment. Equation (2) provides a generalized calculation for the cumulative adjustment:

$$A_{t_x} = O_{t_0} + [O_{t_1} + D_{t_0}(t_1 - t_0)] + \dots + [O_{t_x} + D_{t_{x-1}}(t_x - t_{x-1})] \quad (2)$$

where A is the cumulative adjustment, O is adjustment for offset, D is adjustment for drift, and t is the time in years since deployment. Conditioning the DuraFET sensors in flowing seawater for a few weeks prior to deployment leads to improved sensor stability and smaller initial offsets [Bresnahan *et al.*, 2014; Johnson *et al.*, 2016], and this method has been adopted for all SOCCOM float deployments from 2016 forward. Three of the four floats analyzed here (floats 9254, 9031, and 9096) were not conditioned prior to deployment, and as a result, the adjustments that have been made to these pH sensors are larger than the current typical adjustments (see Figure S1 in the supporting information).

While many empirical methods exist for estimating seawater TA, we use estimates from a SOCCOM-specific Southern Ocean algorithm (based on T , S , P , O_2 , and location; see supporting information for fit equation and Table S1 for fit coefficients) for this analysis. Another option for alkalinity estimation is LIAR (Locally Interpolated Alkalinity Regression) [Carter *et al.*, 2016], which uses data from the Global Ocean Data Analysis Project (GLODAP) data set [Key *et al.*, 2004] through 1999, with global resolution. The SOCCOM-specific algorithm is a more simple MLR, with one set of coefficients for the entire Southern Ocean determined using discrete bottle samples from recent (2007 to present) Southern Ocean Climate Variability and Predictability and GO-SHIP repeat hydrographic cruises. LIAR and the SOCCOM-specific algorithm employ the same set of predictor variables, and TA estimates generally agree to within their standard uncertainties (6.5 and 4.7 $\mu\text{mol kg}^{-1}$, respectively). For the following analysis an average standard uncertainty in TA of 5.6 $\mu\text{mol kg}^{-1}$ is used.

3. Contributions to Uncertainty in Calculated $\text{pCO}_{2\text{sw}}$ (pH, TA)

To estimate the uncertainty in $\text{pCO}_{2\text{sw}}$ estimated from pH and TA, $\text{pCO}_{2\text{sw}}$ (pH, TA), calculated from a float-based pH measurement and an algorithm estimate of TA, we consider the contributions to uncertainty from three

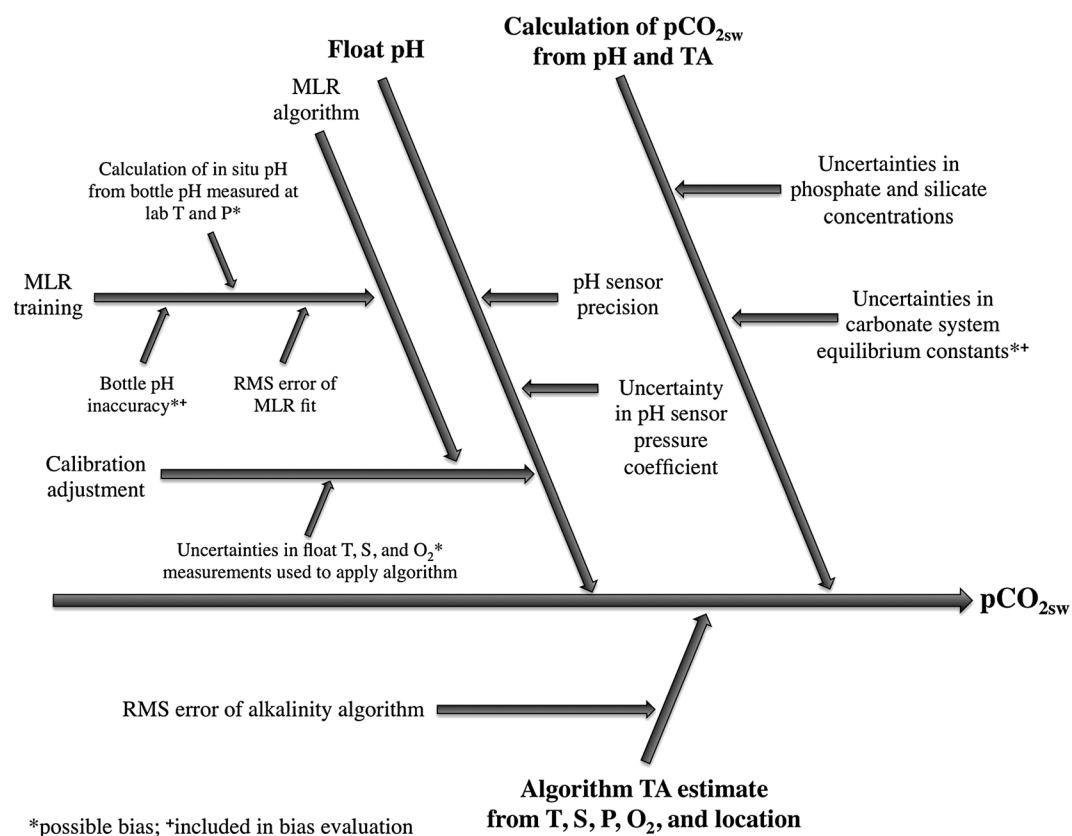


Figure 2. Diagram of contributions to the uncertainty in float-calculated $p\text{CO}_{2\text{sw}}$ (pH, TA) using float pH and an algorithm TA estimate.

main components: (1) float-measured pH, (2) algorithm-estimated TA, and (3) the silicate and phosphate concentrations and carbonate system equilibrium and solubility constants used in the calculation. Figure 2 diagrams the sources of uncertainty with asterisks indicating sources that could lead to a bias in the results and plus signs indicating sources that will be considered in a separate bias assessment. Uncertainties leading to biases will be considered differently than random uncertainties because a bias leads to a larger error in calculated annual air-sea fluxes. Absolute uncertainties are expressed as values, and relative uncertainties are expressed as percentages relative to $\text{pH}=8$, $\text{TA}=2300\ \mu\text{mol kg}^{-1}$, and $p\text{CO}_{2\text{sw}}=400\ \mu\text{atm}$ (e.g., absolute uncertainty of $5\ \mu\text{mol kg}^{-1}$ is 0.2% relative uncertainty in TA). The word “standard” with an uncertainty estimate indicates that the value is expressed as a standard deviation with a confidence interval based on the normal distribution curve. After detailing each source of uncertainty, we calculate an overall uncertainty in float $p\text{CO}_{2\text{sw}}$ (pH, TA) using a Monte Carlo error analysis.

3.1. Float pH

For float-measured pH, there are uncertainty contributions from instrumental precision and from the calibration adjustment process. For the calculation of $p\text{CO}_{2\text{sw}}$ (pH, TA), *Dickson and Riley* [1978] estimated that a 1% change in the hydrogen ion concentration (0.004 in pH) results in a 1.2% change in $p\text{CO}_{2\text{sw}}$ (pH, TA), and we use this sensitivity factor to convert uncertainties in pH to uncertainties in $p\text{CO}_{2\text{sw}}$ (pH, TA) in Table 2. The DuraFET pH sensor has a standard precision of 0.003 based on consecutive pH measurements through a well-mixed surface layer at $\text{pH}\approx 8$ [Martz *et al.*, 2010; Johnson *et al.*, 2016], which converts to 0.9% relative uncertainty in $p\text{CO}_{2\text{sw}}$ (pH, TA). During initial calibration, the responses of each DuraFET pH sensor as a function of T and P are characterized in a laboratory setting [Johnson *et al.*, 2016]. The uncertainty in the T coefficient is negligible, and the uncertainty in the P coefficient equates to a pH uncertainty of 0.0025, resulting in 0.8% uncertainty in $p\text{CO}_{2\text{sw}}$ (pH, TA). As shown in Figure 2, the pH sensor calibration adjustment process introduces additional uncertainty stemming from the MLR algorithm. The MLR algorithm used to adjust the pH sensor is determined using bottle measurements of pH, S , and O_2 and CTD measurements of

Table 2. Summary of Uncertainties in $p\text{CO}_{2\text{sw}}$

	Standard Uncertainty in Parameter	Resulting Relative Uncertainty in $p\text{CO}_{2\text{sw}}$	Absolute Uncertainty at $p\text{CO}_{2\text{sw}} = 400 \mu\text{atm}$ (μatm)	Accounted for in Top- Down Bias Assessment?
pH sensor precision	0.0030	0.9%	3.6	
Uncertainty in pH sensor resulting from uncertainty in pressure coefficient	0.0025	0.8%	3.0	
RMS error of MLR pH introduced through calibration	0.0040	1.2%	4.8	
Bottle pH inaccuracy ^a introduced through calibration	0.0047	1.4%	5.6	yes
Lab to in situ pH conversion uncertainty introduced through calibration	0.0050	1.5%	6.0	
Uncertainty in float O_2 sensor measurements introduced through calibration	0.3%	0.4%	1.6	
Uncertainty in float S sensor measurements introduced through calibration	0.01	0.01%	0.0	
Uncertainty in float T sensor measurements introduced through calibration	0.002	0.005%	0.0	
Uncertainty in estimated Alkalinity	$5.6 \mu\text{mol kg}^{-1}$	0.24%	1.0	
% uncertainty in K_0 ^b	0.50	0.50%	2.0	yes
% uncertainty in K_1	1.73	1.71%	6.8	yes
% uncertainty in K_2	3.45	0.72%	2.9	yes

^aFrom Carter *et al.* [2013].^bFrom Dickson and Riley [1978].

T and P . The root-mean-square error (RMSE) of the MLR fit residuals in pH is 0.004 [Williams *et al.*, 2016], and the absolute uncertainty in the bottle pH measurements used to determine the algorithm is 0.0047 [Carter *et al.*, 2013]. Because the pH algorithm is determined using bottle pH data that were analyzed at lab T and P and converted to in situ conditions at 1500 m, the uncertainty introduced by this conversion must also be considered. The uncertainties in this lab-to-in situ conversion are not well quantified, but a 0.005 uncertainty is likely realistic at the ocean surface [A. Dickson, personal communication, 2016].

An additional possible source of uncertainty in pH originates from uncertainties in the float T , S , and O_2 measurements, which are required for the MLR used for pH sensor calibration adjustments. The uncertainties in the T and S data used in the application of the MLR algorithm are on the order of 0.002°C and 0.01 , respectively [Owens and Wong, 2009]. When the algorithm is applied, the resulting pH uncertainties from the T and S terms (0.00001 and 0.0018, respectively) are several orders of magnitude smaller than the other uncertainties at hand. For Aanderaa O_2 optodes mounted on floats Johnson *et al.* [2015] found no significant drift after float deployment, whereas Bushinsky *et al.* [2016] found, on average, a $0.3\% \text{yr}^{-1}$ drift and recommended adjusting the O_2 sensor gain correction factor over time using ongoing float-based surface air- O_2 measurements. A $0.3\% \text{yr}^{-1}$ drift in O_2 , if left uncorrected, would propagate through as a 0.4% bias in calculated $p\text{CO}_{2\text{sw}}$ (pH, TA) over one year. Most SOCCOM floats obtain an air- O_2 measurement every 10 days, but floats that spend time under ice may not get an air- O_2 measurement for over half a year. To be conservative, we assume that floats will be recalibrated using an air- O_2 measurement at minimum once per year and a 0.4% relative uncertainty contribution in $p\text{CO}_{2\text{sw}}$ (pH, TA) from the O_2 sensor is included in this analysis.

3.2. Estimated Alkalinity

The uncertainty contribution by TA in the calculation of $p\text{CO}_{2\text{sw}}$ (pH, TA) can be approximated by multiplying the relative uncertainty in the TA estimate, 0.24% ($5.6 \mu\text{mol kg}^{-1}$ out of $2300 \mu\text{mol kg}^{-1}$), by the $\% \partial p\text{CO}_2 / \% \partial \text{TA}$ scaling factor, 1.0, given by Dickson and Riley [1978]. The result is a relative uncertainty in $p\text{CO}_{2\text{sw}}$ (pH, TA) of 0.24% or an absolute uncertainty of $1 \mu\text{atm}$ at a $p\text{CO}_{2\text{sw}}$ of $400 \mu\text{atm}$. $p\text{CO}_{2\text{sw}}$ (pH, TA) is mostly dependent on the pH and is less sensitive to TA; therefore, the choice of TA algorithm is relatively unimportant for this application. Of note is that because both LIAR and the SOCCOM-specific algorithm are primarily based on austral summer data, the uncertainties in estimated TA are likely increased when the algorithms are applied throughout the full seasonal cycle and under sea ice, where the processes affecting alkalinity are not as well understood. However, even a doubling of the uncertainty in TA in wintertime would result in just a $1 \mu\text{atm}$

increase in the absolute uncertainty in $p\text{CO}_{2\text{sw}}$ (pH, TA), which is small compared to the other uncertainties involved in the calculation.

3.3. Carbonate System Equilibrium Constants and Nutrient Concentrations

The carbonate system solubility and equilibrium constants (K_0 , K_1 , and K_2), which describe the solubility of CO_2 and dissociation of the carbonate species in seawater as a function of T and S , are determined in laboratory studies, and each carries its own uncertainty. Several sets of equilibrium constants are available for use in carbonate system calculations, and the choice of constants may introduce a bias in $p\text{CO}_{2\text{sw}}$ (pH, TA) [Wanninkhof *et al.*, 1999]. Here we use the equilibrium constants of Lueker *et al.* [2000] as recommended by A. Dickson [Wanninkhof *et al.*, 2016a] because, given the choice of pH on the total scale, they provide the most consistent intercomparison for the four measurable carbonate system parameters [Patsavas *et al.*, 2015]. The estimated uncertainty in K_0 from Dickson and Riley [1978] (based on Weiss [1974]) and estimates of the uncertainties in K_1 and K_2 are used to estimate their contributions to uncertainty in $p\text{CO}_{2\text{sw}}$ (pH, TA). The percent change in $p\text{CO}_{2\text{sw}}$ per percent change in each dissociation constant, K , ($\% \partial p\text{CO}_2 / \% \partial K_x$ scaling factor) given by Dickson and Riley [1978] is multiplied by the estimated standard relative uncertainty in K for each of the three equilibrium constants (Table S2), and the results are included in Table 2.

Concentrations for silicate and phosphate are required for carbonate system calculations because they represent another acid base system in seawater. However, since the floats do not measure these parameters, they are estimated using a subset of Southern Ocean data from the GLODAPv1 database [Key *et al.*, 2004] as a function of potential density. The difference in $p\text{CO}_{2\text{sw}}$ (pH, TA) calculated using zero concentrations or using maximum concentrations of silicate and phosphate is around $0.6 \mu\text{atm}$; thus, they do not contribute appreciably to the bias and uncertainty.

Table 2 summarizes the sources of uncertainty described thus far.

3.4. Top-Down Bias Assessment

Calculating $p\text{CO}_{2\text{sw}}$ (pH, TA) from floats allows the use of the data to calculate F_{CO_2} , which can then be integrated over time to calculate annual net oceanic CO_2 fluxes in the Southern Ocean. After integration, the contribution to the uncertainty in estimated CO_2 uptake by random uncertainties in $p\text{CO}_{2\text{sw}}$ (pH, TA) for any one float will decrease as the number of samples increases, while any biases (i.e., systematic uncertainties) in $p\text{CO}_{2\text{sw}}$ (pH, TA) will remain constant and potentially lead to significant errors in F_{CO_2} . Several of the uncertainties described thus far (marked with asterisks in Figure 2) are systematic. Generally, if the direction and magnitude of a bias is unknown, it should be added to the sum of the other uncertainties. However, if the direction and magnitude of a bias is known, it can be corrected, and then it is only necessary to account for the uncertainty associated with the bias correction [CITAC and Eurachem, 2012]. Here the direction of each individual bias is not explicitly known. However, the following top-down assessment shows that several of these biases (marked as “yes,” accounted for in top-down bias assessment in Table 2 and with a plus sign in Figure 2) partially offset one another and allows the combined overall bias to be characterized.

The equilibrium constants used in this study [Lueker *et al.*, 2000] were derived to optimize the consistency between laboratory measurements of DIC, TA, and $p\text{CO}_{2\text{sw}}$ across a range of seawater conditions. However, this derivation did not include any direct spectrophotometric measurements for pH. As a result, there is a difference between $p\text{CO}_{2\text{sw}}$ (pH, TA) and either directly measured $p\text{CO}_{2\text{sw}}$ or $p\text{CO}_{2\text{sw}}$ (DIC, TA), although the latter two roughly match each other. This difference in $p\text{CO}_{2\text{sw}}$ (pH, TA) can be traced back to differences between pH measured spectrophotometrically and pH calculated from measured DIC and TA as described by Figure 2 of Carter *et al.* [2013]. A similar pattern was observed for the two cruises that were used to quality control the SOCCOM float pH sensor data [Sabine *et al.*, 2012; Talley *et al.*, 2015], where spectrophotometric pH is low relative to pH (DIC, TA) at lower pH and the opposite at high pH (Figure 3). This means that the SOCCOM pH data must be adjusted according to equation (3) below prior to calculating $p\text{CO}_{2\text{sw}}$ (pH, TA) if the result is to be consistent with direct measurements of $p\text{CO}_{2\text{sw}}$.

$$\text{bias correction} = -0.034529 \times \text{pH}(25^\circ\text{C}) + 0.26709 \quad (3)$$

The SOCCOM floats are quality controlled at 1500 m depth where pH (25°C , 0 dbar) averages ~ 7.58 in the Southern Ocean. According to the empirical equation (3) derived from the cruise bottle data, the float pH values are on average 0.0054 low relative to pH (DIC, TA) at this pH, which would lead to about a 1.6%

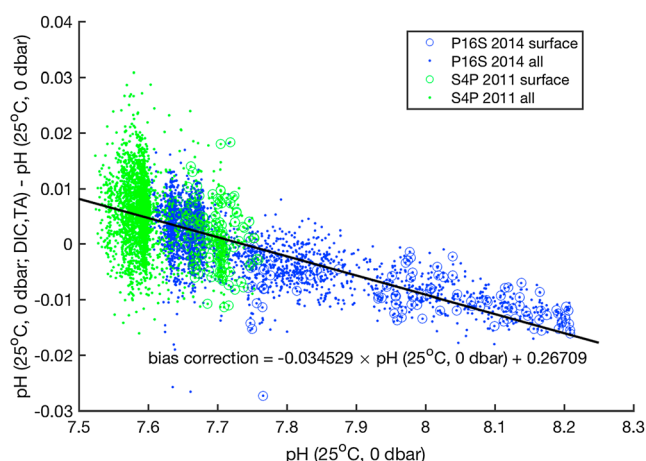


Figure 3. The difference between pH_T (25°C, 0 dbar) measured spectrophotometrically and pH_T (DIC, TA) plotted as a function of pH_T (25°C, 0 dbar) for the two GO-SHIP/SOCCOM deployment cruises used to quality control the float pH sensor data.

Table 2, which accounts for the nonlinear nature of the carbonate system. The Monte Carlo error analysis involves modeling the uncertainty in calculated $\text{pCO}_{2\text{sw}}$ (pH, TA) when the input parameters are varied randomly around their values by their respective uncertainties. The uncertainties associated with the equilibrium constants and the bottle inaccuracy in pH (marked as “yes,” accounted for in top-down bias assessment in Table 2) will not be included in the analysis, but in their place we will use the RMSE of Figure 3 line of best fit (0.0053) as mentioned above. One thousand iterations of calculated $\text{pCO}_{2\text{sw}}$ (pH, TA) are performed for each float profile over the full lifetimes of four SOCCOM floats (9254, 9031, 9096, and 9099). These floats span several frontal regions and represent a wide range of ocean conditions.

4. Results

After correction for known biases (marked as “yes,” accounted for in top-down bias assessment in Table 2) and running the Monte Carlo error analysis with the remaining uncertainties, the combined relative standard uncertainty of 2.7% (11 μatm at $\text{pCO}_{2\text{sw}}$ of 400 μatm) represents the 68% confidence level of biogeochemical float-based $\text{pCO}_{2\text{sw}}$ (pH, TA) estimates in the Southern Ocean. This work focuses on surface $\text{pCO}_{2\text{sw}}$ estimates and does not consider the additional uncertainties that may be introduced when these calculations are done subsurface.

To evaluate our uncertainty estimate, surface float $\text{pCO}_{2\text{sw}}$ (pH, TA) are compared with shipboard underway $\text{pCO}_{2\text{sw}}$ measurements [Sutherland *et al.*, 2015, 2016; van Heuven *et al.*, 2016; Wanninkhof *et al.*, 2016b] from the time and location of float deployment (Figure 4) using both the uncorrected (open circles) and the bias-corrected (solid squares) float results. The underway $\text{pCO}_{2\text{sw}}$ data were matched by date, time, and location ($\pm 0.01^\circ$ latitude and longitude) to the float deployment calibration CTD cast. The underway $\text{pCO}_{2\text{sw}}$ data have a 1% relative uncertainty [Takahashi *et al.*, 2009], and because $\text{pCO}_{2\text{sw}}$ is highly temperature dependent, the underway $\text{pCO}_{2\text{sw}}$ data are adjusted to float T using CO2SYS [Lewis and Wallace, 1998; van Heuven *et al.*, 2011] in combination with float-based estimates of TA, silicate, and phosphate. The uncorrected and bias-corrected float data are both on average biased high relative to the underway data by 7.2 and 3.7 μatm , respectively. All float $\text{pCO}_{2\text{sw}}$ data move in the same direction after bias correction because all of the floats discussed here are in regions where 1500 m pH is relatively low. The reduction in error between the two data sets indicates that the bias correction outlined in section 3.4 improves the overall agreement between the float and underway $\text{pCO}_{2\text{sw}}$ results and improves the accuracy of float $\text{pCO}_{2\text{sw}}$ (pH, TA).

The remaining bias and scatter in the comparison of float and underway $\text{pCO}_{2\text{sw}}$ could be attributed to a combination of factors. An unknown bias may be introduced to the float pH data during the quality control process as a result of the uncertainties in the effect of pressure on the carbonate system equilibrium constants, which has been measured only once [Culberson and Pytkowicz, 1968]. Also, the float performs its

positive bias in float $\text{pCO}_{2\text{sw}}$ (pH, TA) (6.4 μatm at $\text{pCO}_{2\text{sw}}$ of 400 μatm) relative to a direct measurement of $\text{pCO}_{2\text{sw}}$. To adjust for this bias, the in situ pH for each individual float profile should be adjusted according to the bias correction calculated using equation (3) and the 1500 m pH (25°C, 0 dbar) value for that profile. The RMS error in the regression line shown in Figure 3 is 0.0053, and this uncertainty will be accounted for in the Monte Carlo error analysis that follows.

3.5. Monte Carlo Error Analysis

We use a Monte Carlo error analysis to assess the overall uncertainty due to the sources of error listed in

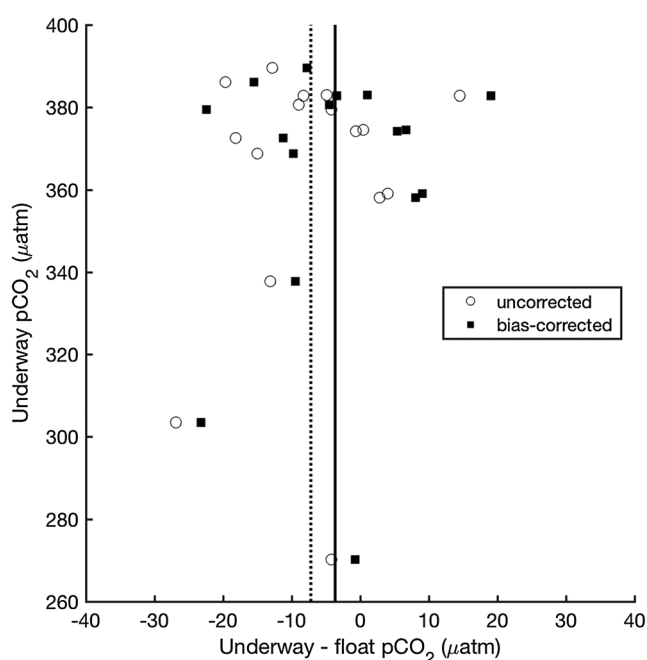


Figure 4. The difference between surface float $p\text{CO}_{2\text{sw}}$ (pH, TA) from the first float profile and shipboard underway $p\text{CO}_{2\text{sw}}$ [Sutherland *et al.*, 2015; Takahashi *et al.*, 2016; van Heuven *et al.*, 2016; Wanninkhof *et al.*, 2016b] at the time and location of the float deployment and calibration CTD cast for 16 SOCCOM floats. Open circles represent the uncorrected float data, and solid squares represent the bias-corrected float data. The average differences for the uncorrected and bias-corrected float data are shown in the dotted and solid lines, respectively.

to regions where wintertime measurements are sparse. Figure 5 shows the calculated $\Delta p\text{CO}_2$ (bias-corrected $p\text{CO}_{2\text{sw}}$ (pH, TA) – $p\text{CO}_{2a}$ from Cape Grim) for four SOCCOM floats representing four different regions: 9254 (WMO ID 5904395) in the subtropical zone, 9031 (WMO ID 5904396) in the subantarctic zone (SAZ), 9096 (WMO ID 5904469) in the polar Antarctic zone, and 9099 (WMO ID 5904468) in the seasonal sea ice zone, with error bars representing 2.7% relative standard uncertainty. The $p\text{CO}_{2a}$ values are adjusted to reflect local sea level pressure at the time of the measurement using National Centers for Environmental Prediction/National Center for Atmospheric Research data available from <http://www.esrl.noaa.gov/psd>. Also plotted are monthly colocated $\Delta p\text{CO}_2$ estimates from Takahashi *et al.* [2014, hereafter T14] and Landschützer *et al.* [2014, 2015, hereafter L14]. For L14, which includes monthly estimates for the years 1982–2011, an average of 2002–2011 was used to create one monthly climatology for this comparison. The RMSEs of the fits to the data from which they were trained are $\pm 10 \mu\text{atm}$ [Takahashi *et al.*, 2009] and $\pm 12 \mu\text{atm}$ [Landschützer *et al.*, 2014]. Positive values will cause a carbon flux out of the ocean and into the atmosphere. Time series of surface in situ float pH and algorithm TA used to calculate $p\text{CO}_{2\text{sw}}$ (pH, TA) for each float can be found in Figure S2.

Directly comparing $p\text{CO}_{2\text{sw}}$ from different years requires adjusting for anthropogenic carbon uptake, which adds uncertainty, so $\Delta p\text{CO}_2$ is used instead of $p\text{CO}_{2\text{sw}}$ to compare the floats with climatologies. Because $p\text{CO}_{2\text{sw}}$ is highly temperature dependent, it is also important to consider differences in SST when comparing values for $p\text{CO}_{2\text{sw}}$ or $\Delta p\text{CO}_2$. A 1°C warming causes a 4.23% increase in $p\text{CO}_{2\text{sw}}$ [Takahashi *et al.*, 1993], which at a $p\text{CO}_2$ near $400 \mu\text{atm}$ is $\sim 17 \mu\text{atm}/^\circ\text{C}^{-1}$. When we compare the float T with SST from the T14 climatology (Figure 6), we observe temperature differences of up to 2°C between the floats and the climatology, but only sometimes can SST differences explain the observed differences in $\Delta p\text{CO}_2$.

Float 9254 (Figure 5a), which is located in the subtropical zone, compares reasonably well with the climatological estimates for $\Delta p\text{CO}_2$ throughout the annual cycle with the exception that the float observes a few anomalously high $\Delta p\text{CO}_2$ values in the summers of 2015 and 2016. A comparison of float 9254 and T14 climatological SST (Figure 6a) reveals that the area where the float surfaced was anomalously warm at those

first profile after drifting at 1000 m depth for approximately 18 h after deployment, and this time and space lag, along with the uncertainty in underway $p\text{CO}_{2\text{sw}}$ measurements, could account for the scatter in the difference between the bias-corrected float and the underway $p\text{CO}_{2\text{sw}}$ values. In the Southern Ocean, drifters and shipboard underway measurements have observed gradients in $p\text{CO}_{2\text{sw}}$ that can range from 5 to $50 \mu\text{atm}$ over scales of 100 km that cannot be fully explained by gradients in sea surface temperature (SST) [Lo Monaco *et al.*, 2014; Resplandy *et al.*, 2014].

5. Discussion

While float-based calculated $p\text{CO}_{2\text{sw}}$ (pH, TA) is inherently more uncertain (2.7% relative uncertainty) than most ship- or mooring-based $p\text{CO}_{2\text{sw}}$ measurements [Takahashi *et al.*, 2009; Bakker *et al.*, 2016], a well-calibrated array of biogeochemical floats can complement the existing global data set by providing a seasonal context

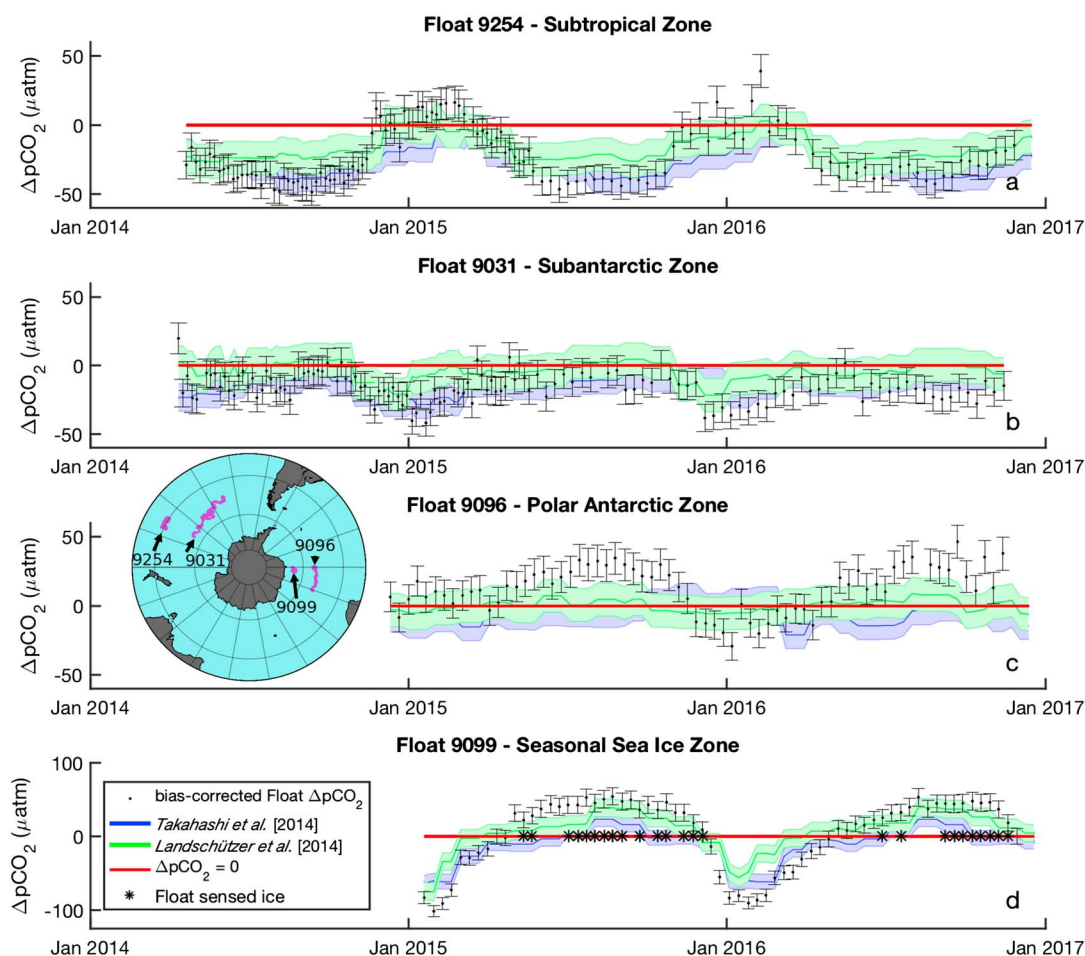


Figure 5. Bias-corrected calculated $\Delta p\text{CO}_{2\text{sw}}$ for SOCCOM floats (a) 9254, (b) 9031, (c) 9096, and (d) 9099 with error bars representing 2.7% relative uncertainty and nearby climatological estimates from Takahashi *et al.* [2014] and the Landschützer *et al.* [2014, 2015] data product (averaged over the years 2002–2011). Positive values indicate carbon flux out of the ocean and into the atmosphere. Inset map shows float locations as of 21 December 2016.

times, and this could explain the summertime differences in $\Delta p\text{CO}_2$. However, there were other times when float 9254 was warmer than the climatological SST but the float did not observe significantly different $\Delta p\text{CO}_2$ from the climatologies.

For float 9031 (Figure 5b), which is just north of the subantarctic front of the Antarctic Circumpolar Current (ACC) in the Pacific sector of the SAZ, calculated $\Delta p\text{CO}_{2\text{sw}}$ matches well with climatological estimates that show the region to be a weak sink for CO_2 throughout the year. The SST observed by the float matches well with the climatological SST (Figure 6b).

In contrast, there is significant disagreement between the climatologies and float 9096, which is located south of the ACC in the Atlantic sector of the polar Antarctic zone (Figure 5c). Both climatological estimates imply a nearly neutral oceanic sink/source for CO_2 , while the float-calculated $\Delta p\text{CO}_2$ is mostly positive, implying that the region occupied by this float was a strong CO_2 source for around two thirds of the year each year. Float 9096 is consistently cooler than the climatological SST (Figure 6c), and this temperature difference alone would cause the float $\Delta p\text{CO}_2$ to be lower than the climatological $\Delta p\text{CO}_2$, but we observe the opposite. The large differences in $\Delta p\text{CO}_2$ between the float and the climatologies occur in winter months when upwelling and entrainment are dominant drivers of surface ocean $p\text{CO}_{2\text{sw}}$. An increase in the strength of the upwelling or an increase in the DIC of the upwelled waters could explain this observed increase in $\Delta p\text{CO}_2$. Williams *et al.* [2015] observed an increase in the DIC of circumpolar deep waters (the source of upwelled waters in this region) of around $12 \mu\text{mol kg}^{-1}$ in the Pacific sector of the Southern Ocean between 1992

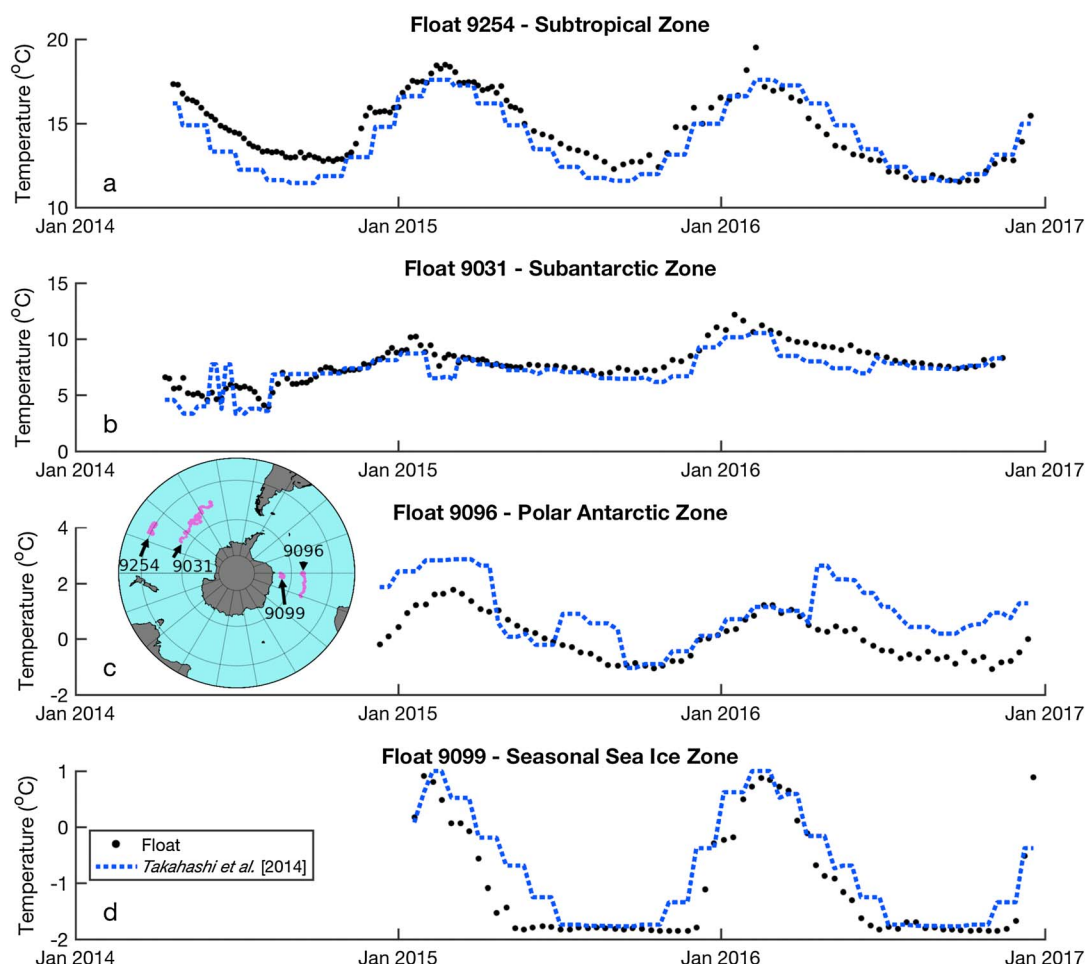


Figure 6. The sea surface temperature measured by the float (black dots) compared with colocated climatological sea surface temperature from *Takahashi et al.* [2014] (blue dashed line). Inset map shows float locations as of 21 December 2016.

and 2011; *Woosley et al.* [2016] and *Wanninkhof et al.* [2010] found similar increases in the Atlantic sector over a similar time period.

Float 9099 (Figure 5d), located in the seasonal sea ice zone in the Atlantic sector and covered by sea ice between May and November, is in better agreement with L14 in both the magnitude of the seasonal cycle and time evolution of $\Delta p\text{CO}_2$ than with the T14 climatology. As with float 9096, the SST observed by the float is lower on average than the climatological T14 SST and explains the summertime but not the wintertime differences in $\Delta p\text{CO}_2$. *Takahashi et al.* [2009] used underway data from six north-south wintertime transects to estimate $p\text{CO}_{2\text{sw}}$ for regions with partial ice coverage as a function of the day of the year and then used this relationship to represent the $p\text{CO}_{2\text{sw}}$ in the entirety of the climatological Antarctic seasonal sea ice zone. The *Takahashi et al.* [2009] relationship ($p\text{CO}_{2\text{sw}} = 0.802 \times \text{day of year} + 208.9$) along the float 9099 track results in T14 $\Delta p\text{CO}_2$ increasing through time until September, and then declining, whereas the float $\Delta p\text{CO}_{2\text{sw}}$ stays positive until October or November, when the ice begins to break up and outgassing and biological draw-down of CO_2 brings $\Delta p\text{CO}_2$ back toward negative values.

In general, the climatologies tend to agree with the floats within their respective uncertainties during the austral summer when there are significantly more underway $p\text{CO}_{2\text{sw}}$ data to create the climatology. Large disagreements arise when there are no suitable data to constrain the climatology, such as austral winter and in ice-covered waters. This disagreement is not surprising, considering (1) the limited availability of austral winter and under ice observations to compute the climatologies and (2) the $p\text{CO}_{2\text{sw}}$ climatologies are based on climatological sea ice cover, which may differ from float observations. L14 attempt to overcome data limitations through the use of a self-organizing map to cluster available $p\text{CO}_{2\text{sw}}$ data into geochemical

provinces, using T , S , mixed layer depth, and climatological $p\text{CO}_{2\text{sw}}$ from Takahashi *et al.* [2009]. These geochemical provinces are allowed to evolve with time, and data from the Southern Ocean seasonal sea ice zone are often combined with data from other similar ocean regions to estimate the L14 $p\text{CO}_{2\text{sw}}$ climatology. However, the disagreements with the float data are similar to that of T14 because the geochemical provinces are constructed, in part, using the same $p\text{CO}_{2\text{sw}}$ data and suffer from wintertime data limitation.

While the calculation of the magnitude of the CO_2 flux relies on several other factors such as wind speed and solubility, which each bring significant additional uncertainties, the direction of the flux at a given time is determined by the sign of $\Delta p\text{CO}_2$. In addition to illuminating the source or sink component of the CO_2 flux in these frontal regions, the float $p\text{CO}_{2\text{sw}}$ (pH, TA) estimates reveal that the magnitude of the seasonal cycles in $p\text{CO}_{2\text{sw}}$ in the subtropical zone, polar Antarctic zone, and seasonal sea ice zone is larger than estimated by currently available climatologies. These biogeochemical floats will also be useful in constraining processes controlling gas flux in partial sea ice coverage because of their capability to sample under sea ice and because the errors in TA estimation are less important than other errors in the $p\text{CO}_{2\text{sw}}$ (pH, TA) calculation. Because these floats have a lifetime of up to 5 years, they can also provide insights into interannual variability in $p\text{CO}_{2\text{sw}}$ and F_{CO_2} and their drivers and provide contrast between various oceanographic regimes as they migrate across fronts and in and out of eddies. An array of floats providing data on 10 day time scales has a strong potential to significantly improve our understanding of the effect that large-scale climate variability has on the air-sea CO_2 flux in the Southern Ocean [Majkut *et al.*, 2014].

Acknowledgments

A snapshot of the quality controlled SOCCOM biogeochemical float data used in this study is available at <http://doi.org/10.6075/J0QC01DJ>. The float temperature and salinity data used in this project are available at <http://doi.org/10.17882/42182> and were made freely available by the International Argo Program and the national programs that contribute to it. Other discrete and underway cruise data used in this study are available at <https://cchdo.ucsd.edu> and <http://cdiac.ornl.gov/oceans>. This work was sponsored by the U.S. National Science Foundation's Southern Ocean Carbon and Climate Observations and Modeling (SOCCOM) project under the NSF award PLR-1425989, supplemented by NASA (NNX14AP49G). Additionally, we acknowledge support from U.S. Argo through NOAA/JISAO grant NA17RJ1232 to the University of Washington. Logistical support for this project in Antarctic waters was provided by the U.S. National Science Foundation through the U.S. Antarctic Program and the U.S. GO-SHIP program, Australia's CSIRO, and Germany's Alfred Wegener Institute. Richard Feely was supported by the Ocean Observations and Monitoring Division, Climate Program Office, National Oceanic and Atmospheric Administration, U.S. Department of Commerce. Work done at Monterey Bay Aquarium Research Institute was supported by the David and Lucile Packard Foundation. Alison Gray was supported by a NOAA Climate and Global Change postdoctoral fellowship. Nancy Williams is also supported by the ARCS Foundation Oregon Chapter. We would like to thank J. Plant, A. Fassbender, and B. Carter for helpful discussions, and we gratefully acknowledge Are Olsen and an anonymous reviewer for insightful comments that have strengthened this manuscript. This is PMEL contribution number 4547.

6. Conclusions

Ongoing shipboard and moored observation programs show that the $p\text{CO}_{2\text{sw}}$ is increasing globally as a result of anthropogenic emissions. Nonetheless, our current understanding of the seasonal cycle and interannual variability, and thus the mechanisms controlling $p\text{CO}_{2\text{sw}}$ and air-sea CO_2 flux, is lacking over many parts of the world ocean. Despite the estimated 2.7% relative standard uncertainty in current biogeochemical float-based $p\text{CO}_{2\text{sw}}$ (pH, TA) estimates, it is clear from the differences between existing climatologies and new float pH-based $p\text{CO}_{2\text{sw}}$ (pH, TA) estimates that incorporating information from these novel carbon observational platforms can improve climatologies, climate models, and future projections. While true space/time cross-overs between biogeochemical floats and shipboard $p\text{CO}_2$ systems are rare, and spatial and temporal heterogeneity make direct comparisons difficult, we have shown that a well-calibrated biogeochemical float provides meaningful data that strengthen the current body of $p\text{CO}_{2\text{sw}}$ observations.

Maintaining a well-calibrated biogeochemical float array for estimating carbonate system parameters relies on high-quality shipboard measurements of pH and oxygen to anchor the sensor data at deployment and float-based air oxygen measurements to adjust the float calibration beyond the initial deployment cast. While early SOCCOM floats exhibited pH sensor drift and relied heavily upon the MLR algorithms for calibration adjustments, the pH sensors deployed during the 2015/2016 field season equilibrated with natural seawater prior to deployment [Bresnahan *et al.*, 2014; Johnson *et al.*, 2016] show no sign of significant drift to date as compared with the empirical algorithms. As float-based sensors continue to improve, the uncertainties in float-based $p\text{CO}_{2\text{sw}}$ (pH, TA) estimates should decrease. However, the uncertainty in calculated $p\text{CO}_{2\text{sw}}$ (pH, TA) resulting from uncertainties in the carbonate system equilibrium and solubility constants will likely remain. Due to the significant value added, well-calibrated float pH-based $p\text{CO}_{2\text{sw}}$ (pH, TA) along with other derived variables, such as aragonite and calcite saturation state, should be included in future data compiling efforts and climatological estimates while taking into account the estimated uncertainty in these calculated quantities. We believe that this uncertainty analysis will aid in the consideration and planning for a future global biogeochemical array [Johnson and Claustre, 2016].

References

- Bakker, D. C. E., *et al.* (2016), A multi-decade record of high-quality $f\text{CO}_2$ data in version 3 of the Surface Ocean CO_2 Atlas (SOCAT), *Earth Syst. Sci. Data*, 8, 297–323, doi:10.5194/essd-2016-15.
- Bresnahan, P. J., T. R. Martz, Y. Takeshita, K. S. Johnson, and M. LaShomb (2014), Best practices for autonomous measurement of seawater pH with the Honeywell Durafet, *Methods Oceanogr.*, 9, 44–60, doi:10.1016/j.mio.2014.08.003.
- Bushinsky, S. M., S. R. Emerson, S. C. Riser, and D. D. Swift (2016), Accurate oxygen measurements on modified Argo floats using in situ air calibrations, *Limnol. Oceanogr. Methods*, 14(8), 491–505, doi:10.1002/lom3.10107.

- Carter, B. R., J. A. Radich, H. L. Doyle, and A. G. Dickson (2013), An automated system for spectrophotometric seawater pH measurements, *Limnol. Oceanogr. Methods*, *11*, 16–27, doi:10.4319/lom.2013.11.16.
- Carter, B. R., N. L. Williams, A. R. Gray, and R. A. Feely (2016), Locally interpolated alkalinity regression for global alkalinity estimation, *Limnol. Oceanogr. Methods*, *14*(4), 268–277, doi:10.1002/lom.3.10087.
- CITAC, and Eurachem (2012), *Quantifying Uncertainty in Analytical Measurement*, 3rd ed., edited by S. L. R. Ellison and A. Williams, EURACHEM, London.
- Culberson, C., and R. M. Pytkowicz (1968), Effect of pressure on carbonic acid, boric acid and the pH in seawater, *Limnol. Oceanogr.*, *13*(3), 403–417.
- Dickson, A. G. (1990), Standard potential of the reaction: $\text{AgCl(s)} + 1/2 \text{H}_2\text{(g)} = \text{Ag(s)} + \text{HCl(aq)}$, and the standard acidity constant of the ion HSO_4^- in synthetic sea water from 273.15 to 318.15 K, *J. Chem. Thermodyn.*, *22*(2), 113–127, doi:10.1016/0021-9614(90)90074-Z.
- Dickson, A. G., and J. P. Riley (1978), The effect of analytical error on the evaluation of the components of the aquatic carbon-dioxide system, *Mar. Chem.*, *6*(1), 77–85, doi:10.1016/0304-4203(78)90008-7.
- Frölicher, T. L., J. L. Sarmiento, D. J. Paynter, J. P. Dunne, J. P. Krasting, and M. Winton (2015), Dominance of the Southern Ocean in anthropogenic carbon and heat uptake in CMIP5 models, *J. Clim.*, *28*(2), 862–886, doi:10.1175/JCLI-D-14-00117.1.
- Johnson, K. S., and H. Claustre (2016), Bringing biogeochemistry into the Argo age, *Eos*, *97*, doi:10.1029/2016EO062427.
- Johnson, K. S., J. N. Plant, S. C. Riser, and D. Gilbert (2015), Air oxygen calibration of oxygen optodes on a profiling float array, *J. Atmos. Oceanic Technol.*, *32*(11), 2160–2172, doi:10.1175/JTECH-D-15-0101.1.
- Johnson, K. S., H. W. Jannasch, L. J. Coletti, V. A. Elrod, T. R. Martz, Y. Takeshita, R. J. Carlson, and J. G. Connery (2016), Deep-Sea DuraFET: A pressure tolerant pH sensor designed for global sensor networks, *Anal. Chem.*, *88*(6), 3249–3256, doi:10.1021/acs.analchem.5b04653.
- Key, R. M., A. Kozyr, C. L. Sabine, K. Lee, R. Wanninkhof, J. L. Bullister, R. A. Feely, F. J. Millero, C. Mordy, and T. H. Peng (2004), A global ocean carbon climatology: Results from Global Data Analysis Project (GLODAP), *Global Biogeochem. Cycles*, *18*, GB4031, doi:10.1029/2004GB002247.
- Landschützer, P., N. Gruber, D. C. E. Bakker, and U. Schuster (2014), Recent variability of the global ocean carbon sink, *Global Biogeochem. Cycles*, *28*, 927–949, doi:10.1002/2014GB004853.
- Landschützer, P., N. Gruber, and D. C. E. Bakker (2015), An observation-based global monthly gridded sea surface pCO_2 product from 1998 through 2011 and its monthly climatology, *Global Biogeochem. Cycles*, doi:10.3334/CDIAC/OTG.SPCO2_1982_2011_ETH_SOM-FFN.
- Le Quéré, C., et al. (2016), Global Carbon Budget 2016, *Earth Syst. Sci. Data*, *8*(2), 605–649, doi:10.5194/essd-8-605-2016.
- Lee, K., T.-W. Kim, R. H. Byrne, F. J. Millero, R. A. Feely, and Y.-M. Liu (2010), The universal ratio of boron to chlorinity for the North Pacific and North Atlantic oceans, *Geochim. Cosmochim. Acta*, *74*(6), 1801–1811, doi:10.1016/j.gca.2009.12.027.
- Lewis, E., and D. W. R. Wallace (1998), *Program Developed for CO_2 System Calculations*, Carbon Dioxide Information Analysis Center, Oak Ridge Natl. Lab., U.S. Dep. of Energy, Oak Ridge, Tenn.
- Lo Monaco, C., N. Metzl, F. D'Ovidio, J. Lloret, and C. Ridame (2014), Rapid establishment of the CO_2 sink associated with Kerguelen's bloom observed during the KEOPS2/OISO20 cruise, *Biogeosci. Discuss.*, *11*(12), 17,543–17,578, doi:10.5194/bgd-11-17543-2014.
- Lueker, T. J., A. G. Dickson, and C. D. Keeling (2000), Ocean pCO_2 calculated from dissolved inorganic carbon, alkalinity, and equations for K_1 and K_2 : Validation based on laboratory measurements of CO_2 in gas and seawater at equilibrium, *Mar. Chem.*, *70*(1–3), 105–119, doi:10.1016/S0304-4203(00)00022-0.
- Majkut, J. D., B. R. Carter, T. L. Frölicher, C. O. Dufour, K. B. Rodgers, and J. L. Sarmiento (2014), An observing system simulation for Southern Ocean carbon dioxide uptake, *Philos. Trans. R. Soc. London, Ser. A*, *372*(2019), 20130046, doi:10.1098/rsta.2013.0046.
- Martz, T. R., J. G. Connery, and K. S. Johnson (2010), Testing the Honeywell Durafet® for seawater pH applications, *Limnol. Oceanogr. Methods*, *8*(5), 172–184, doi:10.4319/lom.2010.8.172.
- Owens, W. B., and A. P. S. Wong (2009), An improved calibration method for the drift of the conductivity sensor on autonomous CTD profiling floats by θ -S climatology, *Deep Sea Res., Part I*, *56*(3), 450–457, doi:10.1016/j.dsr.2008.09.008.
- Patsavas, M. C., R. H. Byrne, R. Wanninkhof, R. A. Feely, and W.-J. Cai (2015), Internal consistency of marine carbonate system measurements and assessments of aragonite saturation state: Insights from two U.S. coastal cruises, *Mar. Chem.*, *176*, 9–20, doi:10.1016/j.marchem.2015.06.022.
- Perez, F. F., and F. Fraga (1987), Association constant of fluoride and hydrogen ions in seawater, *Mar. Chem.*, *21*(2), 161–168, doi:10.1016/0304-4203(87)90036-3.
- Resplandy, L., J. Boutin, and L. Merlivat (2014), Observed small spatial scale and seasonal variability of the CO_2 system in the Southern Ocean, *Biogeosciences*, *11*(1), 75–90, doi:10.5194/bg-11-75-2014.
- Sabine, C. L., R. A. Feely, R. Wanninkhof, A. G. Dickson, F. J. Millero, D. A. Hansell, and J. H. Swift (2012), Carbon dioxide, hydrographic, and chemical data obtained during the R/V Nathaniel B. Palmer Cruise in the Southern Ocean on CLIVAR Repeat Hydrography Section 504P (Feb. 19–Apr. 23, 2011), Carbon Dioxide Inf. Anal. Cent., Oak Ridge Natl. Lab., U.S. Dep. of Energy, Oak Ridge, Tenn.
- Sutherland, S. C., T. Newberger, T. Takahashi, and C. Sweeney (2015), Report of underway pCO_2 measurements in surface waters and the atmosphere during March–May 2014 R/V Nathaniel B. Palmer Cruise 14/3, Lamont-Doherty Earth Observatory of Columbia Univ., Palisades, New York.
- Sutherland, S. C., T. Newberger, T. Takahashi, and C. Sweeney (2016), Report of underway pCO_2 measurements in surface waters and the atmosphere during December 2015 R/V Nathaniel B. Palmer Cruise 15/11, Lamont-Doherty Earth Observatory of Columbia Univ., Palisades, New York.
- Takahashi, T., J. Olafsson, J. G. Goddard, D. W. Chipman, and S. C. Sutherland (1993), Seasonal variation of CO_2 and nutrients in the high-latitude surface oceans: A comparative study, *Global Biogeochem. Cycles*, *7*(4), 843–878, doi:10.1029/93GB02263.
- Takahashi, T., et al. (2009), Climatological mean and decadal change in surface ocean pCO_2 , and net sea–air CO_2 flux over the global oceans, *Deep Sea Res., Part II*, *56*(8–10), 554–577, doi:10.1016/j.dsr2.2008.12.009.
- Takahashi, T., S. C. Sutherland, D. W. Chipman, J. G. Goddard, and C. Ho (2014), Climatological distributions of pH, pCO_2 , total CO_2 , alkalinity, and CaCO_3 saturation in the global surface ocean, and temporal changes at selected locations, *Mar. Chem.*, *164*, 95–125, doi:10.1016/j.marchem.2014.06.004.
- Takahashi, T., S. C. Sutherland, and A. Kozyr (2016), *Global Ocean Surface Water Partial Pressure of CO_2 Database: Measurements Performed During 1957–2015 (Version 2015)*, ORNL/CDIAC-160, NDP-088(V2015), Carbon Dioxide Information Analysis Center, Oak Ridge Natl. Lab., U.S. Dep. of Energy, Oak Ridge, Tenn.
- Talley, L. D., R. A. Feely, A. G. Dickson, J. H. Swift, C. A. Carlson, M. Warner, A. P. McNichol, R. M. Key, and P. Schlosser (2015), *Carbon Dioxide, Hydrographic, and Chemical Data Obtained During the R/V Nathaniel B. Palmer Repeat Hydrography Cruises in the Pacific Ocean: GO-SHIP Sections P16S_2014 (20 March–5 May, 2014)*, Carbon Dioxide Information Analysis Center, Oak Ridge Natl. Lab., U.S. Dep. of Energy, Oak Ridge, Tenn.

- van Heuven, S., D. Pierrot, J. W. B. Rae, E. Lewis, and D. W. R. Wallace (2011), *MATLAB Program Developed for CO₂ System Calculations. ORNL/CDIAC-105b*, Carbon Dioxide Information Analysis Center, Oak Ridge Natl. Lab., U.S. Dep. of Energy, Oak Ridge, Tenn.
- van Heuven, S., M. Hoppema, and O. Boebel (2016), *Surface Measurements of pCO₂ Data Obtained During the SOCCOM Float Deployment Expedition Onboard R/V Polarstern Cruise ANTXXX_2 (2 December 2014–1 February 2015)*, Carbon Dioxide Information Analysis Center, Oak Ridge Natl. Lab., U.S. Dep. of Energy, Oak Ridge, Tenn.
- Wanninkhof, R., E. Lewis, R. A. Feely, and F. J. Millero (1999), The optimal carbonate dissociation constants for determining surface water pCO₂ from alkalinity and total inorganic carbon, *Mar. Chem.*, 65(3–4), 291–301, doi:10.1016/S0304-4203(99)00021-3.
- Wanninkhof, R., S. C. Doney, J. L. Bullister, N. M. Levine, M. Warner, and N. Gruber (2010), Detecting anthropogenic CO₂ changes in the interior Atlantic Ocean between 1989 and 2005, *J. Geophys. Res.*, 115, C11028, doi:10.1029/2010JC006251.
- Wanninkhof, R., et al. (2016a), *An Evaluation of pH and NO₃ Sensor Data From SOCCOM Floats and Their Utilization to Develop Ocean Inorganic Carbon Products: A Summary of Discussions and Recommendations of the Carbon Working Group (CWG) of SOCCOM*, Princeton Environmental Institute, Princeton, N. J.
- Wanninkhof, R., K. Sullivan, and D. Pierrot (2016b), *Underway pCO₂ Measurements in Surface Waters and the Atmosphere During the R/V Roger Revelle GO-SHIP Cruise Along the Section I08S_2016 (February 8–March 15, 2016)*, Carbon Dioxide Information Analysis Center, Oak Ridge Natl. Lab., U.S. Dep. of Energy, Oak Ridge, Tenn.
- Weiss, R. F. (1974), Carbon dioxide in water and seawater: The solubility of a non-ideal gas, *Mar. Chem.*, 2(3), 203–215, doi:10.1016/0304-4203(74)90015-2.
- Williams, N. L., R. A. Feely, C. L. Sabine, A. G. Dickson, J. H. Swift, L. D. Talley, and J. L. Russell (2015), Quantifying anthropogenic carbon inventory changes in the Pacific sector of the Southern Ocean, *Mar. Chem.*, 174, 147–160, doi:10.1016/j.marchem.2015.06.015.
- Williams, N. L., L. W. Juranek, K. S. Johnson, R. A. Feely, S. C. Riser, L. D. Talley, J. L. Russell, J. L. Sarmiento, and R. Wanninkhof (2016), Empirical algorithms to estimate water column pH in the Southern Ocean, *Geophys. Res. Lett.*, 43, 3415–3422, doi:10.1002/2016GL068539.
- Woosley, R. J., F. J. Millero, and R. Wanninkhof (2016), Rapid anthropogenic changes in CO₂ and pH in the Atlantic Ocean: 2003–2014, *Global Biogeochem. Cycles*, 30, 70–90, doi:10.1002/2015GB005248.